Mon. Not. R. Astron. Soc. **289**, 745–752 (1997)

NGC 6749: a metal-poor halo globular cluster in a disc field rich in Mira variables

L. Rosino,[1] S. Ortolani,[2] B. Barbuy[3] and E. Bica[4]

[1] *Osservatorio Astronomico di Padova, Dept di Astronomia, Vicolo dell'Osservatorio 5, I-35122 Padova, Italy*
[2] *Università di Padova, Dept di Astronomia, Vicolo dell'Osservatorio 5, I-35122 Padova, Italy*
[3] *Universidade de São Paulo, IAG, Dept de Astronomia, CP 9638, São Paulo 01065-970, Brazil*
[4] *Universidade Federal do Rio Grande do Sul, Dept de Astronomia, CP 15051, Porto Alegre, 91500-970, Brazil*

Accepted 1997 May 1. Received 1997 March 17; in original form 1996 July 23

ABSTRACT

We present V, I photometry of the loose star cluster NGC 6749, and for the first time colour–magnitude diagrams are provided. We confirm that it is a globular cluster and its blue horizontal branch indicates that it is metal-poor. We derive a reddening of $E(B-V)=1.39\pm0.04$ and a distance from the Sun $d_{\odot}=7.3\pm0.9$ kpc (assuming a total-to-selective absorption $R=3.4$). The cluster is projected very close to the Galactic plane, and the derived distance implies a Galactic coordinate $Z\approx-300$ pc. It is thus a halo globular cluster located close to the disc plane.

We also discuss the properties of 78 newly discovered long-period variable stars, of which 75 are Miras, projected within 1° of the cluster centre. The variables do not appear to be associated with the globular cluster. From their periods, most of them belong to the metal-rich disc or bulge stellar populations.

Key words: stars: variables: other – globular clusters: individual: NGC 6749 – Galaxy: halo.

1 INTRODUCTION

The present study deals with the star cluster NGC 6749, which is located at $\alpha_{1950}=19^{h}02^{m}43^{s}$, $\delta_{1950}=+01°49'30''$, and is also designated as GCL-107 (Alter et al. 1970) and GCL B1902+0149. Although indicated as a globular cluster in Alter et al., as well as in most of the more recent compilations (e.g. Webbink 1985; Djorgovski 1993), its classification is not obvious. As pointed out by Canterna & Rosino (1981, hereafter CR81), it might be interpreted either as a rich open cluster or as a poor loose globular cluster, being projected close to the Galactic plane ($l=36°.201, b=-2°.205$). Racine (1975 and references therein) called attention to the fact that NGC 6749 may even be a highly reddened young open cluster. Thus very little information is available on the cluster, in particular no colour–magnitude diagram (CMD) has yet been published. CR81 determined a concentration parameter $c=0.75$ from infrared photography, which would place the cluster among the least concentrated globular clusters. From the cosecant law they estimated a reddening of $E(B-V)=1.27$, whereas taking Racine's (1975) integrated UBV photometry, they derived $E(B-V)=1.28$, by assuming an intrinsic colour $(B-V)_0=0.75$. CR81 finally adopted $E(B-V)=1.40$ based also on reddening determinations for neighbouring clusters, and determined an approximate value for the distance modulus $(m-M)_0=15.0$, based on the methods of the 25 brightest stars and Kukarkin's (1974) index of richness. On the other hand, Harris & Racine (1979) estimated a lower reddening $E(B-V)=0.96$ which they marked as uncertain, based on the available integrated colours. The parameters for NGC 6749 listed in the recent compilations are all based on the above-cited early observations, including Webbink's (1985) metallicity value [Fe/H] $=-0.37$. Webbink also estimated a horizontal branch level $V_{HB}=19.2$ and a distance from the Sun $d_{\odot}=12.8$ kpc, which corresponds to a distance modulus $(m-M)_0=15.54$.

In the present work we provide V, I CMDs for NGC 6749 and derive more accurate cluster parameters. We also present photometry in the same filters for the metal-poor M30 (NGC 7099) and the intermediate metallicity NGC 6752 globular clusters, for comparison purposes. CMDs in V and I are not yet widely available in the literature, and such templates with low reddening and located in uncrowded fields are fundamental references for the study of reddened clusters such as NGC 6749.

The direction of the cluster in the Galaxy is particularly interesting because it samples a disc field and possibly the

outer bulge population. In fact, the field is very rich in Miras, which can be used as tracers of stellar populations, and the results of a deep plate survey in the near-infrared (*I* band) of variable stars in the cluster field are also presented.

In Section 2 the CCD photometry is described. In Section 3 the CMDs are discussed and the cluster parameters are derived. In Section 4, variables in the cluster field, most of them Miras, are studied. Finally, the concluding remarks are given in Section 5.

2 OBSERVATIONS

The cluster observations were obtained at the European Southern Observatory (ESO), using the 3.55-m New Technology Telescope (NTT) and Danish 1.54-m telescope.

The SUSI camera was used at the NTT, with a 1024 × 1024 thinned Tektronix CCD at the Nasmyth focus B. The pixel size is 24 μm (0.13 arcsec on the sky), and the frame size is 2.2 × 2.2 arcmin^2.

At the Danish telescope we used the Tektronix CCD # 28 of 1024 × 1024 pixels, with pixel size 24 μm (0.37 arcsec pixel^{-1}). The field size is 6.3 × 6.3 arcmin^2. In Fig. 1 the Danish *I* image is shown, in which the sparse cluster structure can be seen.

The Danish observations were taken under photometric conditions, including Landolt (1983, 1992) stars, whereas the NTT data were not photometric. The Danish observations were used to calibrate the zero-point, whereas the colour terms were derived from NTT data from previous nights. The reductions were carried out in the standard way, and the calibration equations (where Landolt stars

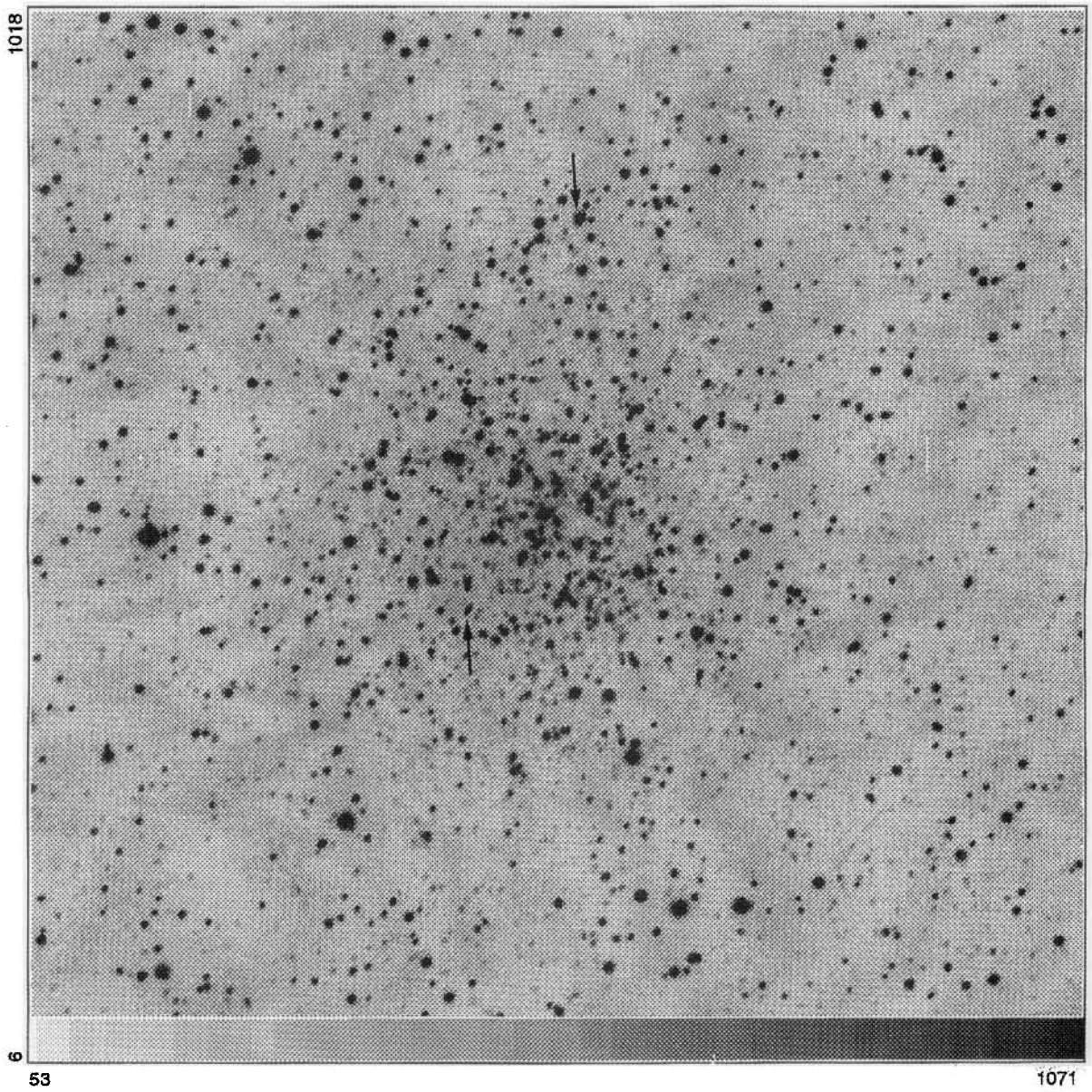

Figure 1. NGC 6749: Danish *I* image with dimensions 6.3 × 6.3 arcmin^2. The variable stars A-1 (upper arrow) and A-2 (lower arrow) are indicated.

were used) are: $V=26.91+0.04(V-I)+v$; $I=26.09+i$ (numbers are for 30-s exposures and airmass of 1.1).

The reduction procedure using DAOPHOT II was described in detail in the Liller 1 study (Ortolani, Barbuy & Bica 1996 and references therein), which was observed in the same run. The main sources of error in the photometry are the zero-point accuracy (± 0.03 mag) and the magnitude transfer from the cluster images to the standard stars, due to the crowded field, which can amount to 0.05 mag. The photometric errors are approximately constant to $I=17.5$, amounting to 0.02 mag; at $I=18.5$ the error increases to 0.07 mag.

The template clusters M30 and NGC 6752 have been observed at the NTT equipped with the EFOSC2 focal reducer. The detector was a Thomson-coated CCD ESO # 17, with 1024×1024 pixels, 19-μm pixel size, with a scale projected on the sky of 0.15 arcsec pixel^{-1}. The total field of view is about 2×2 arcmin^2. Landolt (1983) standards have been observed in the same nights for photometric calibrations.

For comparison with the cluster field, we also observed a field in the antigalactic centre direction ($l=180°$, $b=-3°.5$) using the 2.2-m telescope equipped with EFOSC2, and the Thomson-coated CCD ESO # 19, of 1024×1024, 19-μm pixel size, yielding 0.26 arcsec pixel^{-1}, and a total of 4.3×4.3 arcmin^2.

The log book of these CCD observations is reported in Table 1.

3 COLOUR–MAGNITUDE DIAGRAMS

We show in Fig. 2 a V versus $(V-I)$ diagram for the whole NTT frame (2.2×2.2 arcsec^2). The main CMD features are (i) a vertical red giant branch (RGB) and (ii) a blue clump at $V \approx 19.7$ and $(V-I) \approx 1.9$ suggesting a blue HB, which is, however, substantially contaminated by a blue main sequence (MS).

In Fig. 3(a) we present a V versus $(V-I)$ CMD for an extraction of radius $r<26$ arcsec centred on NGC 6749, where the CMD features become more clearly defined. The high metallicity for NGC 6749 given in Webbink (1985, section 1) can be excluded given the absence of a red HB. In order to constrain the metallicity of NGC 6749, in Figs 3(b) and (c) are shown the CMDs of the templates M30 and NGC 6752 in V versus $(V-I)$, for comparison purposes. These clusters represent two prototype CMD morphologies for metal-poor and intermediate metallicity ([Fe/H]$=-2.13$ and -1.54 respectively, cf. Zinn 1985).

Table 1. Log book of CCD observations.

Target	Filter	Date	Equipment	Exp.(s)	Seeing(FWHM")
NGC 6749	V	17.05.1994	NTT + SUSI	60	0.9
	V			90	1.1
	I			60	0.9
	I			600	1.2
	V	19.05.1994	Danish	60	1.4
	I			30	1.4
M30	V	02.06.1990	NTT + EFOSC2	10	1.0
	I			2	1.0
NGC 6752	V	31.05.1990	NTT + EFOSC2	10	1.2
	I			1	1.0
Anticenter	V	07.12.1991	2.2m + EFOSC2	1200	1.3
	V			60	1.3
	I			600	1.3

The NGC 6749 CMD morphology is more similar to that of the very metal-poor globular cluster M30 rather than to the intermediate metallicity cluster NGC 6752. This is illustrated by the superimposed mean locus of M30 on the NGC 6749 CMD (Fig. 3a), defined within ± 0.035 in $V-I$ (half width of the RGB) and ± 0.22 in V (half width of the HB). Notice the difference of blue HB morphology between M30 and NGC 6752: a blue HB tail like that of NGC 6752 is absent in both M30 and NGC 6749; also, the RGB of M30 is slightly steeper than that of NGC 6752, and that of NGC 6749 appears to be even steeper. This evidence suggests that the metallicity of NGC 6749 should be [Fe/H] ≈ -2.0.

3.1 Field

In Fig. 4 is presented the V versus $(V-I)$ Danish field (6.3×6.3 arcmin^2), in which the field sequences are more pronounced than in Fig. 2. Note also that the CMD in Fig. 2 (NTT) is ~ 2 mag deeper. The disc blue MS becomes dominant over the cluster HB, and the cluster RGB is mixed with field red stars. The stars of $(V-I)>3.5$ are probably metal-rich bulge or inner disc stars; such red stars do not occur in the anticentre field (Fig. 5).

3.2 Reddening and distance

The HB level in the NGC 6749 CMD is located at $V=19.7 \pm 0.15$, and the colour of the RGB at the HB level is $(V-I)=12.65 \pm 0.04$. We calculate the cluster reddening and distance using M30 as a reference, for which the HB level is $V=15.0$, and the colour of the RGB at the HB level is $(V-I)=0.90$ (Fig. 3b). Adopting $E(B-V)=0.04$ for M30 (Zinn 1985), we obtain $E(V-I)=1.85 \pm 0.05$ for NGC 6749; this value converts to $E(B-V)=1.39 \pm 0.04$ using $E(V-I)/E(B-V)=1.33$, suitable for the cluster colours (Dean, Warpen & Cousins 1978), and for $A_V=4.73$ adopting a total-to-selective absorption $R=A_V/E(B-V)=3.4$ (Olson 1975). Adopting for the absolute magnitude of the HB (for a metallicity [Fe/H] $=-2.0$) the value $M_V^{HB}=0.65$ (Buonanno, Corsi & Fusi Pecci 1989), we obtain

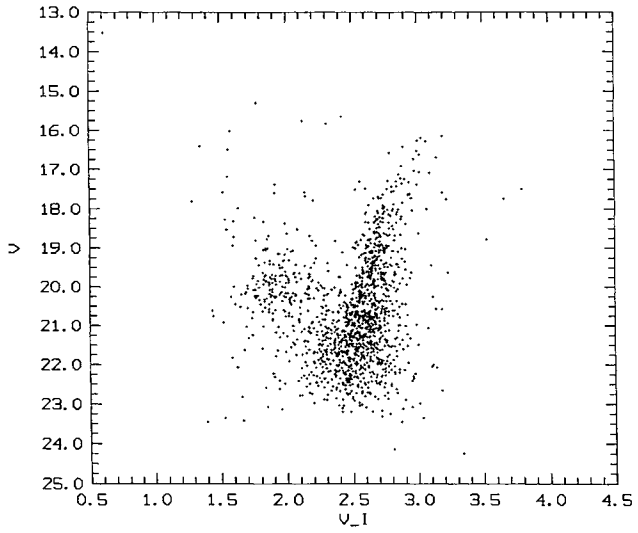

Figure 2. NTT-SUSI V versus $(V-I)$ whole field.

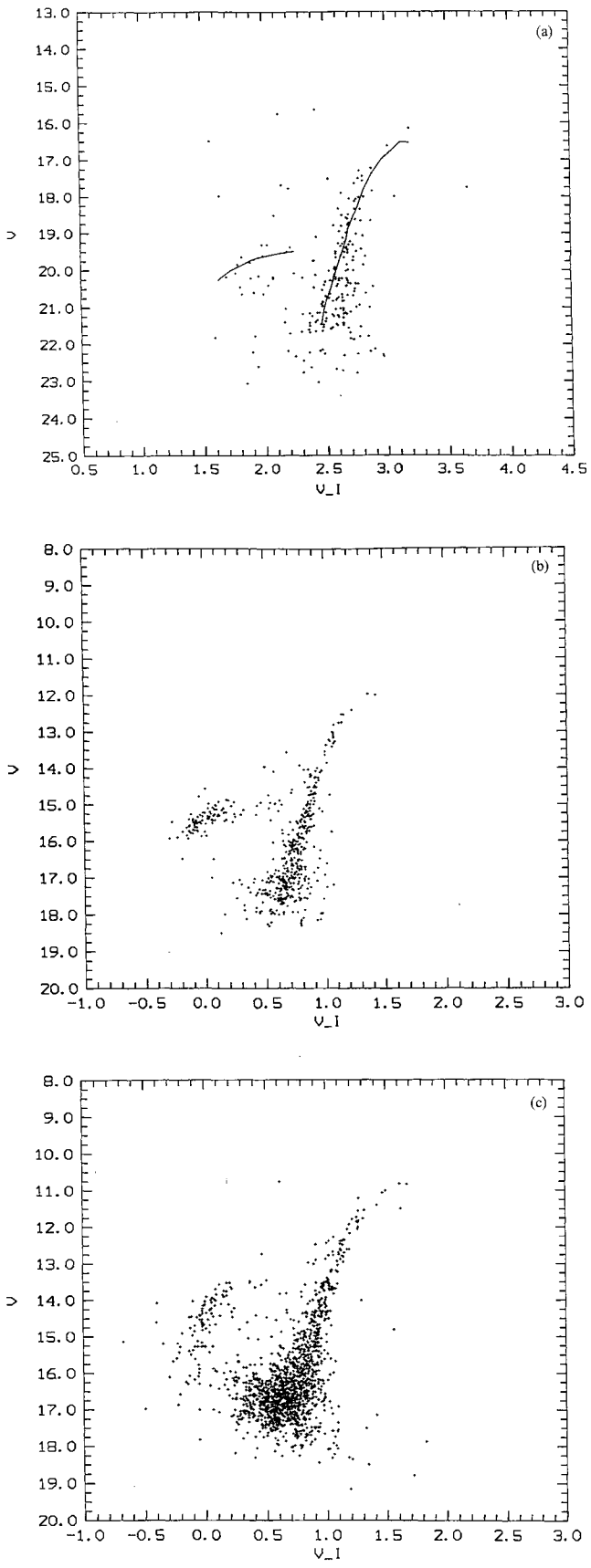

Figure 3. V versus $(V-I)$ for: (a) NGC 6749 extracted for $r<26$ arcsec, where a best fit of the mean locus of M30 is superimposed; (b) M30; (c) NGC 6752.

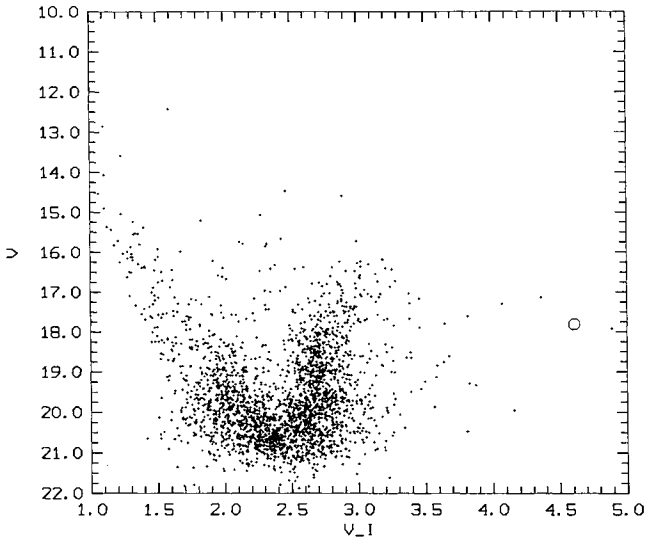

Figure 4. Danish whole frame (6.3×6.3 arcmin^2) including the cluster. Open circle: Mira A-1 (Section 4).

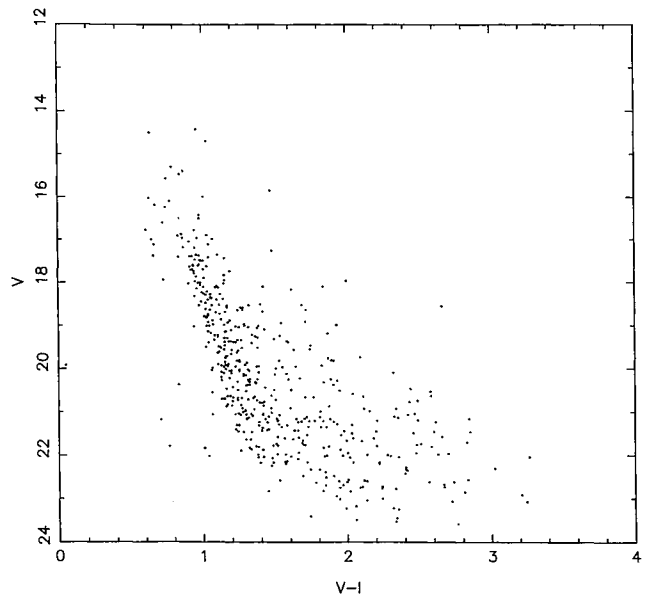

Figure 5. Galactic anticentre ($l=180°$, $b=-3\overset{\circ}{.}5$) field V versus $(V-I)$ CMD.

$(m-M)_0=14.32\pm0.25$ for NGC 6749 and a distance of $d_\odot=7.3\pm0.9$ kpc.

The Galactocentric coordinates of the cluster, assuming a distance of the Sun to the Galactic centre of $R_\odot=8.0$ kpc (Reid 1993), are $X=2.1$ ($X>0$ refers to our side of the Galaxy), $Y=4.3$ kpc and $Z=-0.28$ kpc. The very low metallicity of this cluster is typical of the halo stellar populations; consequently there is the possibility that this cluster is crossing the disc. Kinematical and structural analyses would be interesting for further study of this object.

4 VARIABLE STARS

In the survey of selected Milky Way fields in the search for new Mira variables, carried out at Asiago in the near-

infrared several years ago with the 67–92-cm Schmidt telescope at $l=112°$, $b=0°$ and $l=52°$, $b=2\overset{\circ}{.}7$ (Palomar 10 field) (Rosino, Bianchini & Di Martino 1976; Rosino & Guzzi 1978, respectively), one of us (LR) has studied an area of 30 deg^2, centred on the star cluster NGC 6749. About 300 new variable stars were detected, most of them of Mira type, in addition to the five Mira stars previously known in that direction.

The available material consists of nearly 100 infrared plates (pre-flashed IN + RG5), 30 103a-D + GG14, another 30 103a-O + GG13 and 12 objective-prism plates, all of size 20×20 cm^2 evenly distributed as far as possible, between 1971 and 1985. The temporal distribution of the plates used for the survey excludes the possibility that certain periods may be underrepresented for selection effects for periods longer than 100 d. The plates have been taken in the summer–autumn months of every year from 1971 to 1994. We provide in Table 2 the log book of the photographic data. Long-period variables (LPVs), even those with peculiar periods like 365 d, cannot escape discovery. We illustrate in Fig. 6 representative light curves. We point out that, as far as it concerns LPVs, the search is essentially complete to the plate limit ($I \sim 15.5$–16, $V \approx 18$–18.5) within $1\overset{\circ}{.}0$ from the cluster centre. An amplitude selection effect should be present, affecting to some extent the detection of the variables, because the present research was directed to the discovery of Miras or red LPVs with large amplitudes. A variable can be discovered at the blink only in cases where the difference between two plates is at least 0.5 mag. Since Miras must have at least an amplitude of 1.2 mag, probably

Table 2. Log book of photographic Kodak IN sensitized + RG5 material used for the determination of the periods of Mira stars. N is the number of plates.

Year	Months	N	Mean Interval
1971	Aug – Nov	8	13.1 days
1972	Aug – Nov	8	13.6
1973	Aug – Oct	3	30.0
1974	Jul – Sep	5	13.2
1975	Jun – Oct	2	67.0
1976	Sep – Oct	2	34.0
1977	Jun – Oct	6	23.2
1978	Jun – Oct	5	30.5
1979	Aug – Oct	4	22.7
1980	May – Sep	4	38.3
1981	Jun – Sep	4	31.3
1982	May – Aug	3	43.5
1983	Jun – Oct	6	21.2
1984	Jul – Aug	2	7.0
1985	Jul – Oct	5	21.2
1986	Oct	2	1.0
1988	Aug – Sep	4	13.3
1989	Aug	1	– –
1990	Aug	1	– –
1992	Jul – Sep	3	30.0
1993	May – Aug	5	21.0
1994	Apr – Oct	2	26.0

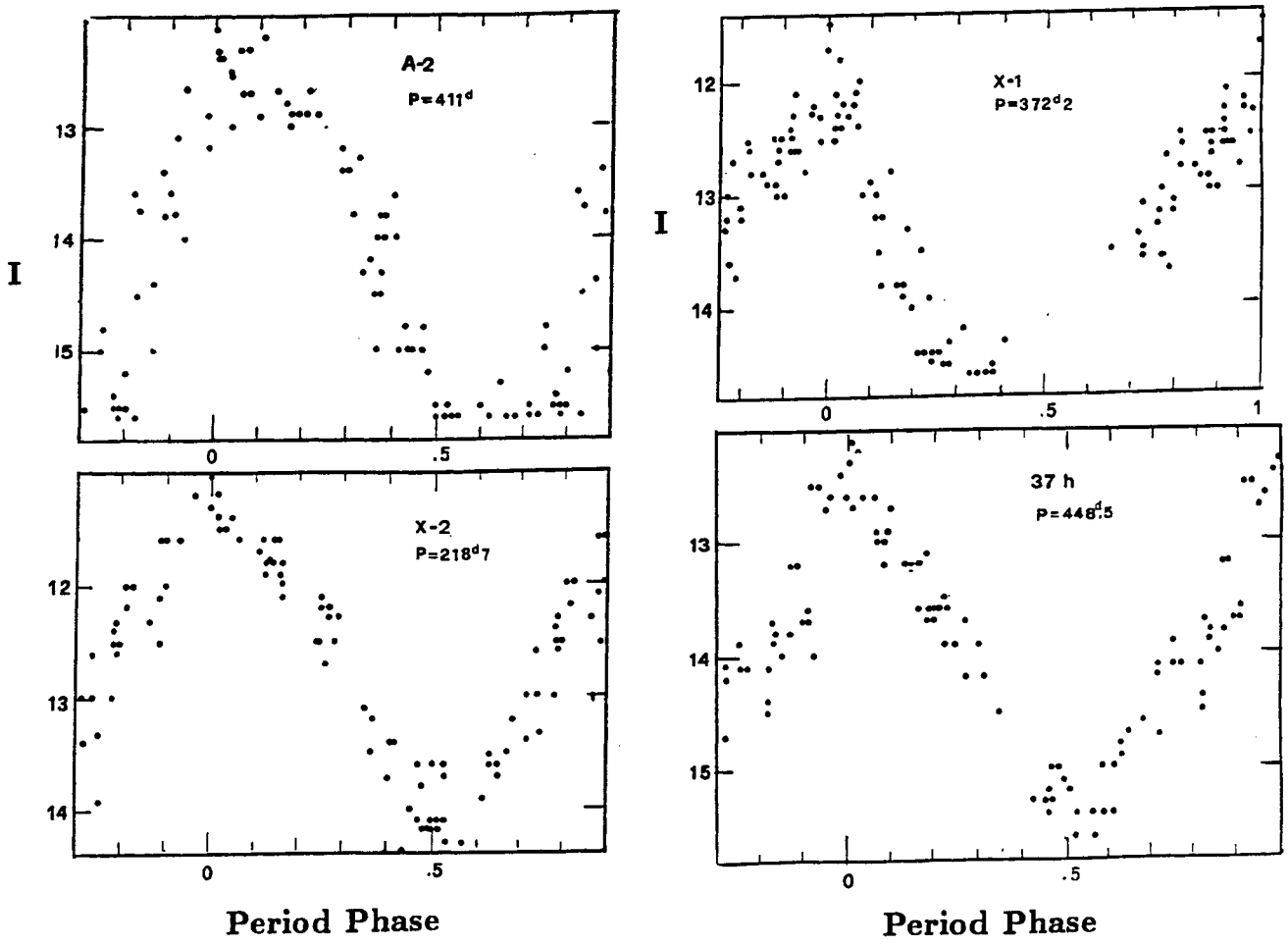

Figure 6. Typical light curves obtained for some Miras: *I* magnitude versus period phase.

Table 3. Mira variables in the NGC 6749 field.[1]

N	α_{1950}	δ_{1950}	T0	P(days)	I_{max}	I_{min}	Notes
			244000+				
95	19 1 06	+2 33.1	1072	237.5	12.8	14.2	
39 = 148	19 1 08	+1 38.1	1112	431.0	12.8	16 :	
63	19 1 37	+2 37.4	1010	349.6	11.5	14.9	
2	19 1 39	+1 54.4	1021	414	12.5	15.5 :	
40 = 15	19 1 46	+1 26.1	1035	257	12.3	14.5	
44	19 1 48	+2 46.7	1206	355.5	11.2	14.4	
3	19 2 03	+2 02.2	902	347.8	11.9	15.0	
151b = 36	19 2 07	+1 17.7	990	290	10.0	13.1	
17	19 2 11	+2 46.5	880	418.0	12.4	15.1	
19	19 2 19	+2 17.9	−−	−−	10.7	11.8	**Irr**
92	19 2 19	+1 27.1	830	428.5	11.3	14.5	
17b	19 2 20	+2 49.6	975	525.5	12.4	15.4 :	
5	19 2 20	+2 28.8	1080	581	11.8	15.2	
7	19 2 22	+2 04.1	1200	479.7	10.9	15.1	
36A	19 2 23	+1 16.9	822	413	11.9	15.8	
4	19 2 23	+2 33.2	1190	439.0	11.9	14.6	
37	19 2 32	+1 11.5	1120	260.3	10.2	14.8	
41	19 2 38	+1 33.4	904	313.5	12.8	15.6	
26	19 2 39	+2 13.4	1185	281.9	11.9	15.1	
6 − 12	19 2 39	+2 09.0	1124	395	11.8	14.0	
91	19 2 43	+1 40.3	2715	328	12.0	15.5	
A − 1	19 2 44	+1 51.4	1143	370	12.1	14.8	
A − 2	19 2 46	+1 49.6	2300	411	12.2	15.6 :	
42	19 2 47	+1 35.0	1180	472.7	9.5	13.0	
27	19 2 49	+2 23.1	1320	465.0	11.8	15.5 :	
10	19 2 50	+1 37.9	1021	579	11.8	15.3	
31b	19 3 26	+2 52.2	1312	512	11.4	15.2	
8	19 3 30	+2 04.1	995	327.8	12.6	15.0	
4 − 3	19 3 31	+1 45.5	1240	375	12.0	15.5	
60 = 37b	19 3 35	+1 17.3	1185	516.5	10.1	13.6	
9	19 3 46	+2 08.0	923	338.8	11.1	14.5	
12	19 3 46	+1 53.2	1030	445	12.5	15.5 :	
37h	19 3 55	+0 55.2	1142	448.5	12.1	15.7	
6 − 6	19 3 58	+3 05.6	1260	207.5	12.0	15.0	
31ter	19 4 10	+3 22.3	1164	432.0	11.4	14.8	
20	19 4 11	+2 57.6	1216	246.5	13.0	15.4	
6 − 4	19 4 14	+3 11.3	1230	398.5	12.9	15.4	
6 − 4b	19 4 16	+3 11.7	1054	314.0	12.9	15.3	
31	19 4 17	+3 20.5	1185	242.8	11.5	14.5	
20c	19 4 26	+2 53.3	1070	431.0	13.1	15.4	
20b	19 4 28	+2 54.4	1205	346.5	12.1	15 :	
51	19 4 29	+1 25.3	932	408.4	11.7	15.2	
81	19 4 31	+2 26.6	1072	336.4	13.2	15.6	
80	19 4 41	+1 12.6	1206	290	10.5	14.2	
30	19 4 43	+3 16.3	1034	306	11.2	14.5	
6 − 2	19 4 44	+3 20.0	1590	365.5	11.8	15.0	
53b	19 4 47	+1 44.6	1206	258.3	11.2	15.5	
X − 2	19 4 55	+2 19.9	1590	218.7	11.0	14.4	
X − 1	19 5 01	+2 29.5	1125	372.2	11.5	14.6	
19 − II	19 5 03	+2 45.4	1660	281.5	11.5	15.3	
32	19 5 08	+3 24.7	1165	231 :	12.6	15.5 :	
82	19 5 36	+2 14.6	1212 :	238.3	12.8	13.8	SR
82b	19 5 36	+2 13.0	959	315.5	12.2	15.5	
18	19 5 37	+2 27.0	1245	188.0	12.4	15.6	
53	19 5 46	+1 41.6	1260	448	11.9	15.5 :	
52b	19 6 02	+1 51.0	1282	347.3	11.9	15.0	
25d	19 6 14	+3 11.0	1100	471	8.7	10.8	SR
52	19 6 17	+1 34.7	1300	382	10.5	14.5	
83	19 6 20	+2 45.7	1250	463.0	12.0	15.5 :	
25	19 6 32	+3 01.5	1165	322.3	12.5	15.2	
33	19 6 47	+2 50.0	1665	296.0	10.4	14.0	
25b	19 7 02	+2 58.3	1295	381.5	12.4	15.2	
22	19 7 10	+2 08.5	1088	294.0	12.2	14.9	
6 − 14	19 7 22	+2 49.7	1090	340	11.6	15.0	
45	19 7 23	+2 41.5	1095	281.5	10.8	14.0	
6 − 14b	19 7 28	+2 46.5	1180	395	13.0	15.2	
0 − 2	19 7 34	+2 57.9	1070	405.5	12.0	16 :	
7 − 1	19 7 36	+3 38.6	1270	311	11.8	14.2	
23	19 7 37	+2 *11*.6	1100	493	12.3	15.5 :	
25e	19 7 39	+3 03.3	1290	335.4	12.0	15.3	
34	19 7 41	+2 39.7	1640	280.0	11.7	15.0	
44c	19 7 50	+2 19.4	1350	352	13.1	15.5	
44b	19 7 52	+2 20.5	1245	318.5	12.8	15.3	
6 − 14*a*	19 7 52	+2 53.1	1132	312.5	12.8	15.5	
24	19 7 54	+2 13.6	1117	236.3	12.3	15.3	
6C	19 8 41	+2 29.8	1131	306.8	13.3	15.5	
6 − 16	19 9 00	+2 45.5	3380	338.5	13.0	15.3	
6d	19 9 30	+2 29.3	−−	449	13 :	15.2 :	

[1] 75 variables are Mira type, 3 are red irregular or semiregular. Three Mira variables already known in the field, namely V810, V1115, and V1192, are not reported in the table.

all Miras brighter than $I=14.5$ at a maximum have been detected in the present survey. Some variables, in particular A-1 and A-2 (Fig. 1) projected on the cluster, were very difficult to detect.

The photographic system defined from the specified filter/plate combination is not a standard system. However, we calibrated it with our Cousins I magnitudes by transfers from selected stars of NGC 6749 (CCD calibrations from Section 2). About 10 uncrowded, very red stars have been used to tie our CCD and the photographic system. No evidence of a trend in colour appeared in our comparison and the errors are within 0.1 mag. Some uncertainties in the zero-point are possible, and other errors in the infrared magnitudes may be due to blends in the crowded cluster and field.

The equatorial coordinates (1950) of the new variables have been determined by measurement (at the PDS microdensitometer) of their positions relative to 27 comparison stars of known coordinates (SAO), well-distributed in the field of the Schmidt plates.

In Table 3 are given: coordinates, T0 (which is the starting date for the phase calculation corresponding to the maximum in Julian days), period in days, I magnitudes (maximum and minimum) of 75 new Mira variables and of three irregular and semiregular stars, which are all those found under the selection procedures described above, within a distance of about 1° from the cluster.

Infrared light curves and finding charts can be obtained under request to LR. The periods (P) have been derived through Fourier analysis with errors less than $0.01P$. The dispersion of the representative points in the mean light curves depends, other than for casual errors in the magnitudes, on the fact that for Mira variables there are minor changes of shape from cycle to cycle.

For eight of them it has been possible to derive the $V-I$ colour index at maximum, as reported in Table 4. At minimum in the V band, most of the Mira stars are invisible ($V \leq 19$–20). From the objective-prism plates it appears that the spectra of the brightest Mira variables are in general of types M5 to M8.

Table 4. Colour indices ($V-I$) of eight variables at maximum light.

N	P	< I >	I_{max}	V_{max}	$< V-I >_{max}$
41	313	14.20	12.8	17.7	+4.9
91	328	13.75	12.0	17.0	+5.0
$A-1$	370	13.45	12.1	17.8	+5.7
$A-2$	411	13.90	12.2	17.8	+5.6
42	473	11.25	9.5	14.8	+5.3
10	579	13.65	11.8	15.5	+3.7
$4-3$	375	13.75	12.0	17.0	+5.0
12	445	14.0	12.5	18.0	+5.5

Table 5. Statistics of the Mira sample (75 stars from Table 3): number of stars in each bin, period bins, mean period, mean amplitude and mean I magnitude.

N	Period(d)	< Period >	< Amplitude >	< I >
3	< 220	204.7	3.20 ± 0.20	13.40 ± 0.66
7	220 – 260	244.2	2.74 ± 0.89	13.61 ± 0.42
9	260 – 300	283.9	3.47 ± 0.54	12.76 ± 0.71
16	300 – 340	322.8	2.81 ± 0.47	13.77 ± 0.52
10	340 – 380	358.1	3.06 ± 0.32	13.44 ± 0.40
11	380 – 420	402.0	3.11 ± 0.69	13.67 ± 0.52
9	420 – 460	439.1	3.02 ± 0.52	13.73 ± 0.53
5	460 – 500	474.7	3.62 ± 0.37	13.11 ± 1.10
3	500 – 540	518.0	3.43 ± 0.40	13.02 ± 1.05
2	540 – 580	580.0	3.45	13.53

Statistical properties for the 75 Miras of Table 3 are presented in Table 5. The number of Miras in period bins reaches the highest value for 300 to 340 d, and it steadily decreases for increasing periods. The periods of Miras are a function of their kinematics and scaleheight, characteristics of the population to which they belong (Feast 1963; Feast, Woolley & Yilman 1972; Whitelock 1995). There may be a lack of shorter period stars in this field compared with the bulge, but this would require confirmation.

The mean I magnitude versus period shown in Fig. 7 indicates a basically flat distribution, as also found by Reid, Hughes & Glass (1995) for the LMC Miras, with a possible excess around $P \approx 280$ d.

The mean I amplitude versus period relation shown in Fig. 8 is flat or at most has a slight trend of increasing amplitudes for increasing periods.

The two Miras A-1 and A-2 identified in Fig. 1 are projected close to the cluster centre. A-2 is extremely red, below detection in the V CCD frames. Since $I=15.99$ at the

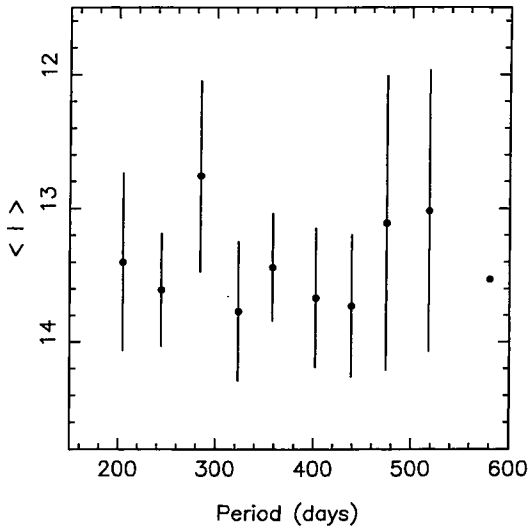

Figure 7. $\langle I \rangle$ versus period relation for the Miras.

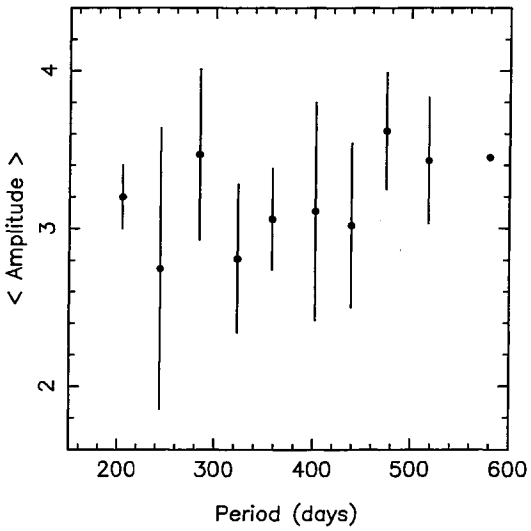

Figure 8. Amplitude versus period distribution for the Miras.

epoch of the CCD observations, and the V limit is ≈ 22.0 in the crowded region of the star, the colour index must be at least $(V-I)=6.0$. This large value places the star at the limit of those of Miras, possibly already evolving as an OH/IR star. The Danish CCD observations give, for the variable A-1, $V=17.8$ and $(V-I)=4.7$. This Mira is in a very crowded location and is a blend in the photographic plates, whereas in the CCD photometry it is resolved. Therefore it appears blue, which explains the difference with the photographic result (Table 3). It is plotted as an open circle in Fig. 4. It falls at the end of the very red field population in that figure, which is also the location of the majority of the newly found Miras.

5 CONCLUDING REMARKS

We have studied the star cluster NGC 6749 with deep CCD photometry, and its surrounding field with Schmidt plates. We have definitely established that it is a globular cluster. The metallicity appears to be comparable to that of M30, one of the most metal-poor globular clusters in the Galaxy. We obtained a reddening of $E(B-V)=1.39$ and a distance $d_{\odot} \approx 7.3$ kpc. We are dealing with a halo globular cluster, presently located at only ≈ 300 pc from the Galactic plane. Kinematical data is needed in order to have information on its orbital motion: given that it is an extremely loose globular cluster, it may be disrupting due to an interaction with the disc.

The field is very rich in long-period variable stars, most of them of Mira type. A catalogue of 78 variables within 1° of the cluster centre, and a statistical analysis of their periods and other properties, were presented. They do not appear to be members of NGC 6749. Most of them have periods longer than 300 d and consequently are to be associated with the metal-rich disc/bulge stellar population.

Finally, the separation of disc and bulge Miras is a key point. The distribution of stars in the Galactic bulge has been shown to be base-shaped, with the near end of the bar in the first quadrant (e.g. Dwek et al. 1995). Miras in the bulge clearly define the bar (Whitelock & Catchpole 1992). The extent of the bulge bar has not yet been determined, but studies of Miras such as those mentioned here might shed some light on the problem. An effort in this direction will be to gather the results of the properties and statistics of Miras in the three fields (Rosino et al. 1976; Rosino & Guzzi 1978; present work) and compare them with results for bulge fields.

ACKNOWLEDGMENTS

We are grateful to an anonymous referee for important comments on an earlier version of this paper.

This paper is based on observations collected at the European Southern Observatory.

REFERENCES

Alter G., Ruprecht J., Vanysek V., 1970, in Alter G., Balazs B., Ruprecht J., eds, Catalogue of star clusters and associations. Akademiai Kiado, Budapest
Blanco V. M., McCarthy M. F. S. J., Blanco B. M., 1984, AJ, 89, 636
Buonanno R., Corsi C. E., Fusi Pecci F., 1989, A&A, 216, 80
Canterna R., Rosino L., 1981, A&AS, 45, 53 (CR81)
Dean J. F., Warpen P. R., Cousins A. J., 1978, MNRAS, 183, 569
Djorgovski S., 1993, in Djorgovski S., Meylan G., eds, ASP Conf. Ser. 50, Structure and Dynamics of Globular Clusters. Astron. Soc. Pac., San Francisco, p. 373
Dwek E. et al., 1995, ApJ, 445, 716
Feast M. W., 1963, MNRAS, 125, 367
Feast M. W., Woolley R., Yilman N., 1972, MNRAS, 158, 23
Harris W. E., Racine R., 1979, ARA&A, 17, 241
Kukarkin B. V., 1974, The Globular Star Clusters. Nauka, Moscow
Landolt A. U., 1983, AJ, 88, 439
Landolt A. U., 1992, AJ, 104, 340
Olson B. I., 1975, PASP, 87, 349
Ortolani S., Barbuy B., Bica E., 1996, A&A, 306, 134
Racine R., 1975, AJ, 80, 1031
Reid I. N., Hughes S. M. G., Glass I. S., 1995, MNRAS, 275, 331
Reid M., 1993, ARA&A, 31, 345
Rosino L., Guzzi L., 1978, A&AS, 31, 313
Rosino L., Bianchini A., Di Martino D., 1976, A&AS, 24, 1
Webbink R. F., 1985, in Goodman J., Hut P., eds, Proc. IAU Symp. 113, Dynamics of Star Clusters. Reidel, Dordrecht, p. 541
Whitelock P., 1995, in Stobie R. S., Whitelock P., eds, ASP Conf. Ser. 83, Astrophysical Applications to Stellar Pulsation. Astron. Soc. Pac., San Francisco, p. 165
Whitelock P., Catchpole R. M., 1992, in Blitz L., ed., The Center, Bulge and Disc of the Milky Way. Kluwer, Dordrecht, p. 365
Zinn R., 1985, ApJ, 293, 424